Impacts and Future Projections of Climate Change on Hurricanes and Drought in Hawaii

Pao-Shin Chu
Department of Atmospheric Sciences/Hawaii State Climate Office
School of Ocean & Earth Science & Technology
University of Hawaii-Manoa

Joint Climate Change Informational Briefing, Hawaii State Capitol
January 11, 2024

Tropical Cyclone strength and impact on the islands

- Tropical cyclone (TC) is the general term for all type of severe storms that originate over tropical waters:

  tropical depression (the weakest)

  tropical storm (at this stage, the storm gets a name)

  hurricane (the strongest)

- Tropical Depression (TD): 20-33 kts
- Tropical Storm (TS): 34-63 kts (at least 39 mph)
- Hurricane (HU): $\geq$ 64 kts (at least 74 mph), 5 categories (1-5), major hurricanes (cat 3-5): > 96 kts (at least 111 mph)

- Destructive winds, torrential rainfall/flooding, and storm surges. The interaction with mountainous topography enhances high-intensity rainfall and leads to flash flooding and triggers landslides in Hawaii.

- In late November 1982, Kauai suffered major property damage from Hurricane **Iwa** approaching $250 million (1983 dollars). This occurred when the strong 1982/83 El Niño event nearly reached its maximum intensity.

- Ten years later in 1992, **Iniki**, a major hurricane (cat 4), ravaged Kauai and western Oahu with damage of $3.1 billion, which is equivalent to $6 billion in 2021.

- In 2015, a very strong El Niño year and a very active hurricane season, Hawaii was sandwiched by 3 major hurricanes (cat 4) simultaneously, an unprecedented phenomenon.

- In 2018, **Lane**, a major hurricane, caused a serious scare for several days because of its strong intensity (cat 5), slow speed, and close distance to Oahu. Lane also brought fire to Maui, and strong wind, torrential rain (58” in six days), and wildfire to the Big Island.

- Hurricane **Douglas** in July 2020 passed dangerously close to Oahu (just 30 mi).

Hurricane Iniki in September 1992, Kauai

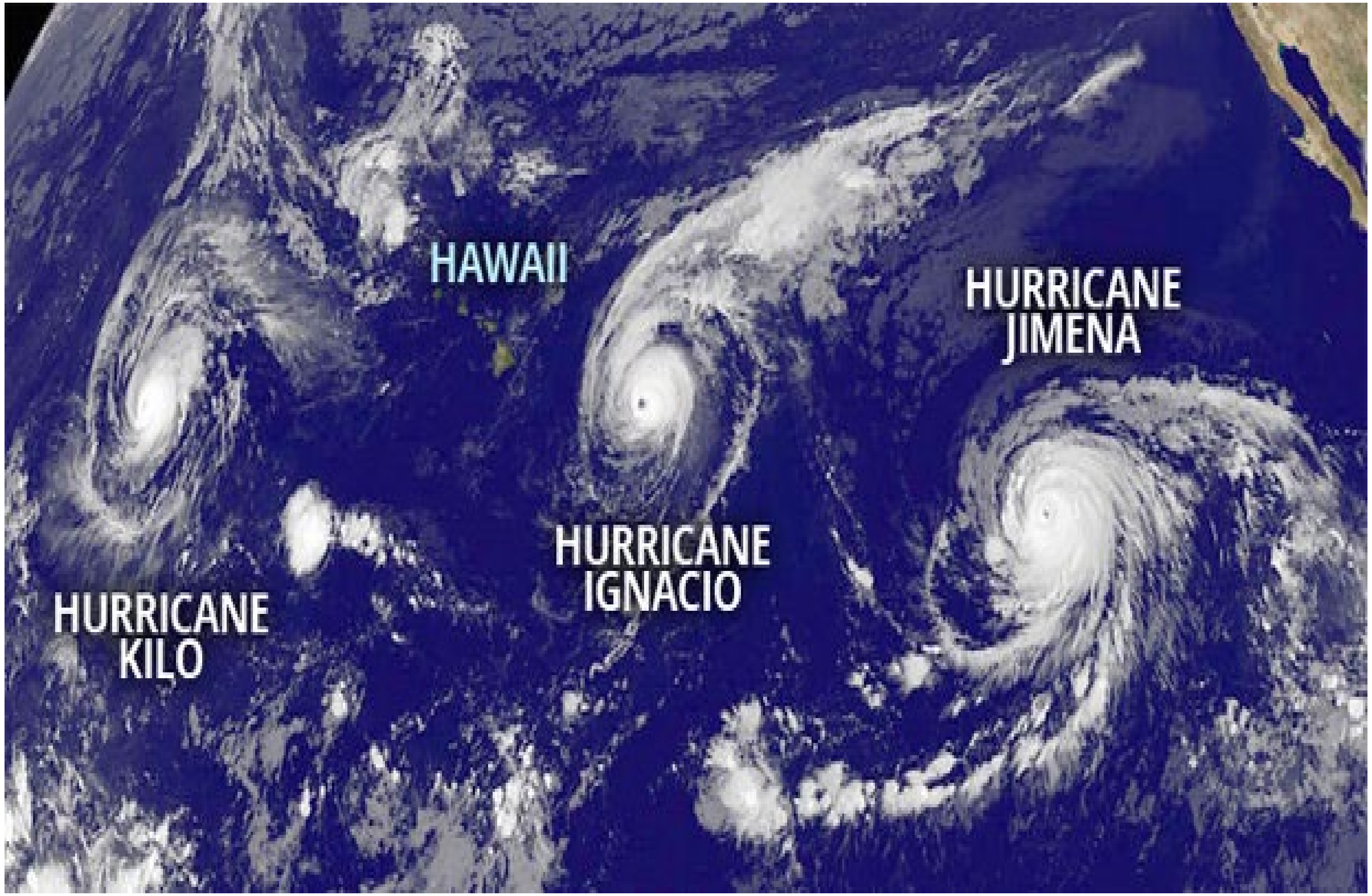

Record-breaking three category 4 hurricanes (major hurricanes) in the central and eastern North Pacific simultaneously on August 30, 2015, a very strong El Niño year. Category 4 hurricanes: one-min sustained wind between 131 and 155 mph. Hawaii was sandwiched by 3 major hurricanes, an unprecedented phenomenon.

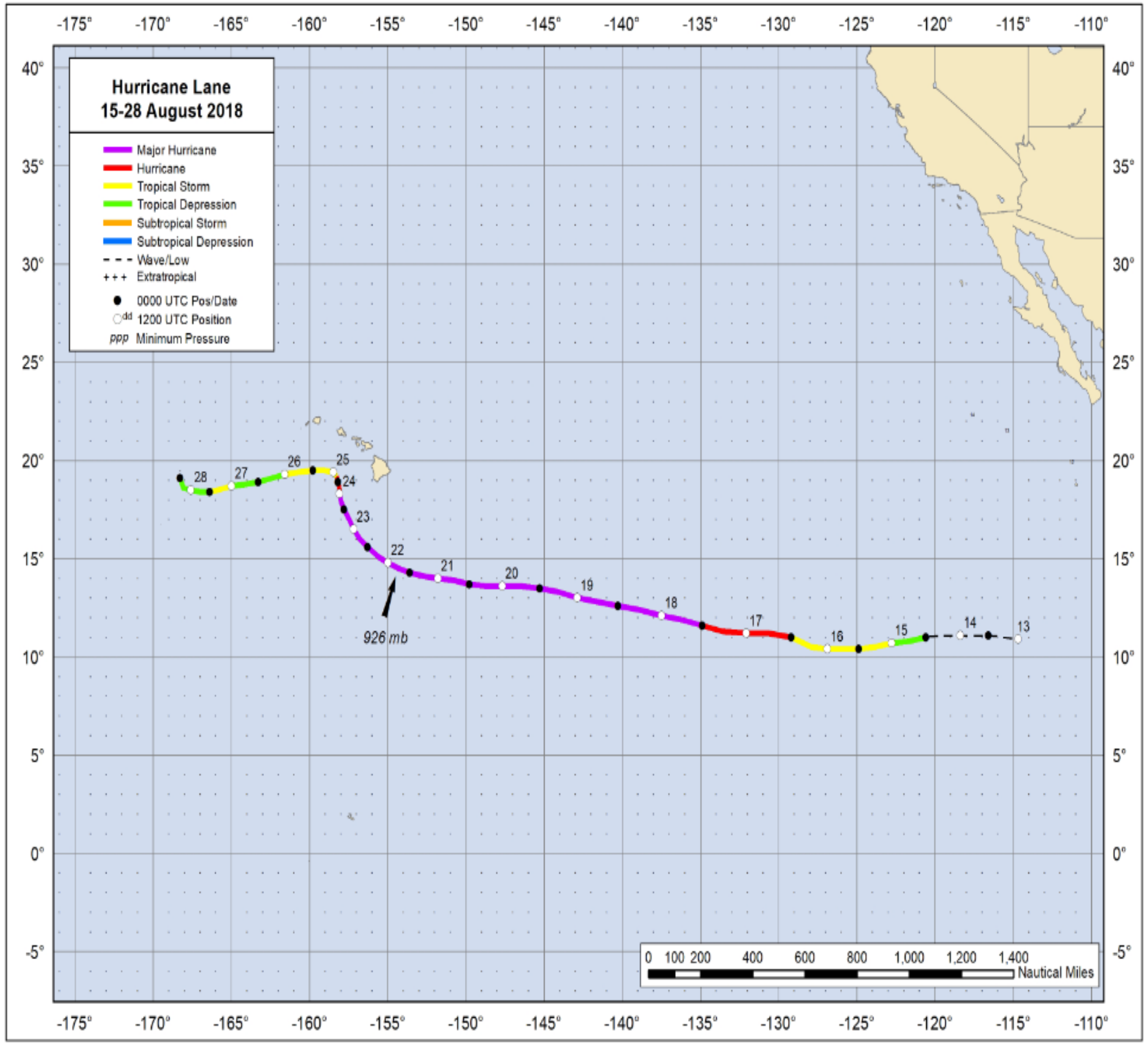

Best track positions for Hurricane Lane, 15–28 August 2018, NWS CPHC. Lane was a category 5 (the strongest) hurricane with 160 mph winds on August 21.

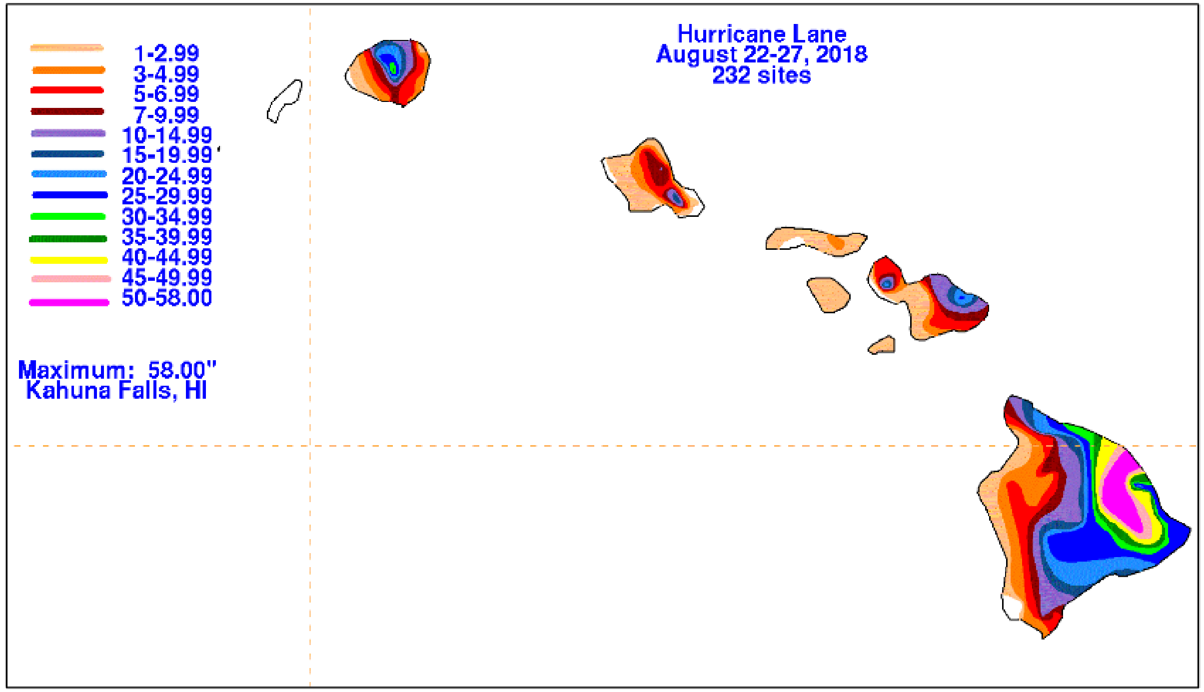

Six-day (August 22-27) rainfall totals (inches) during Hurricane Lane, 2018.

Tropical storm Calvin in July 2023 brought heavy rain and strong winds to the Island of Hawaii.

Passage of Hurricane Dora to the south of Hawaii generated super strong downslope winds (up to 70 mph) on August 8, 2023; fires and power outages occurred on Maui and at least 100 people perished in the blaze of a fast-moving inferno.

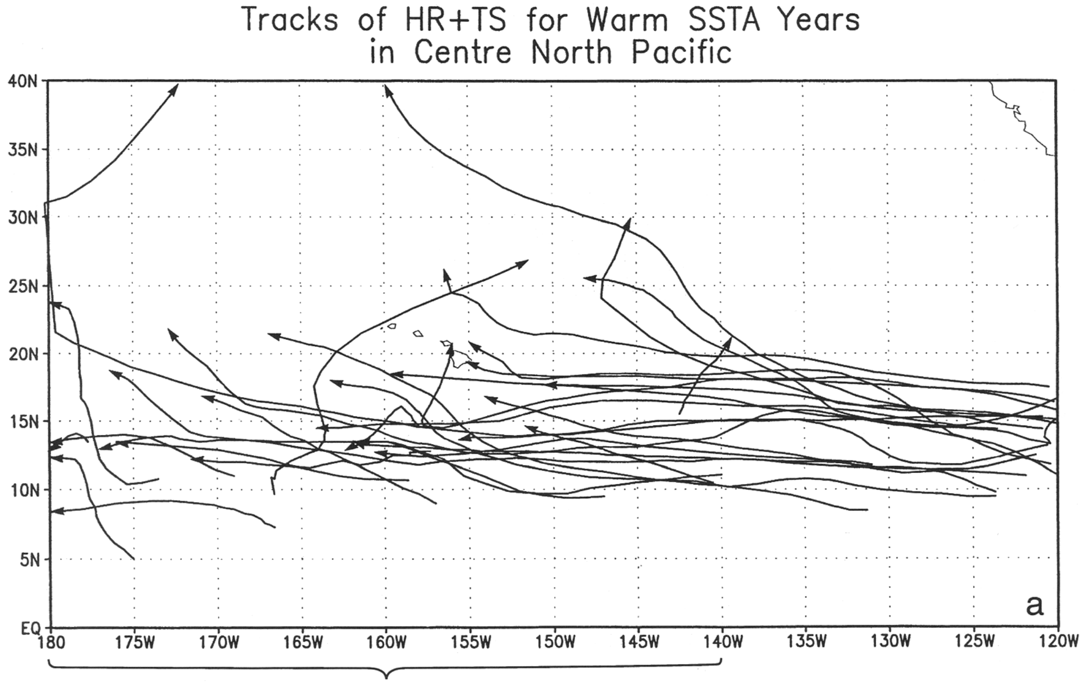

El Nino (6):

33 TCs

14 (42%) formed in the central North Pacific (CNP), defined as a region north of the equator and between 140°W and the Dateline.

19 (58%) moved from the eastern North Pacific (east of 140°W to Americas)

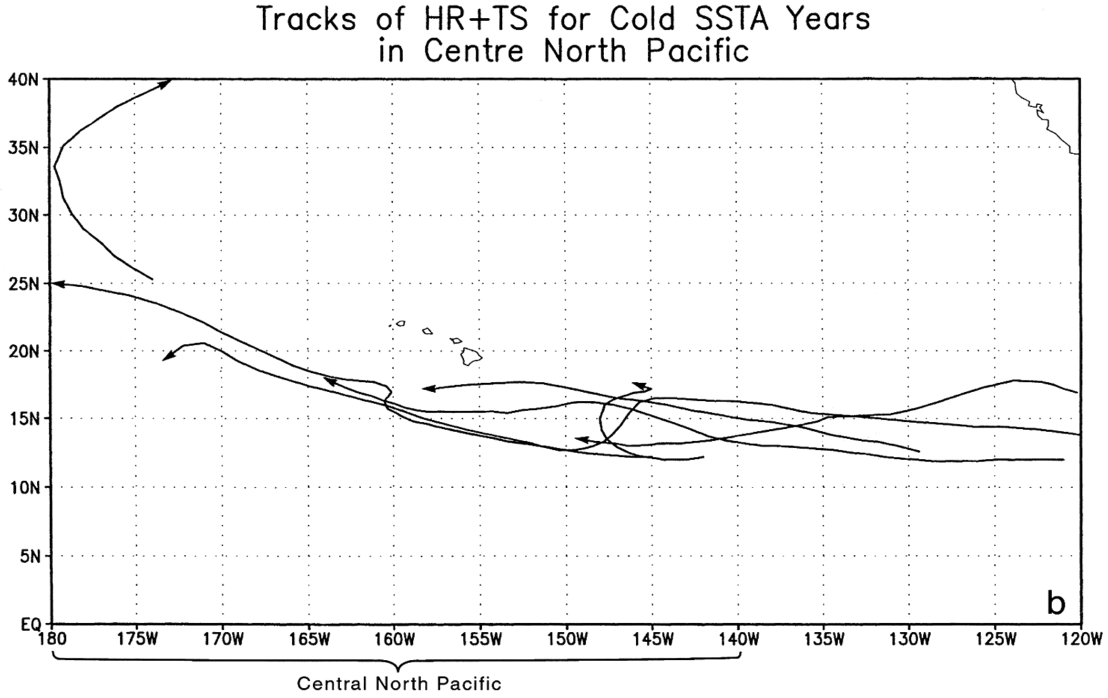

La Nina (4):

7 TCs

1 (14.3%) formed in the CNP

6 (85.7%) moved from ENP

On average, 5.5 TCs are observed over the CNP during El Niño years and only 1.75 TCs during La Niña years, a ratio of 3 to 1.

Tropical Cyclone Occurrences in the Vicinity of Hawaii: Are the Differences between El Niño and Non–El Niño Years Significant?*

PAO-SHIN CHU AND JIANXIN WANG J. Climate

Department of Meteorology, School of Ocean and Earth Science and Technology, University of Hawaii, Honolulu, Hawaii

(Manuscript received 2 January 1997, in final form 7 April 1997)

ABSTRACT

Tropical cyclones in the vicinity of Hawaii are rare. However, when they occurred, they caused enormous property damage. The authors have examined historical records (1949–95) of cyclones and classified them into El Niño and non–El Niño batches. A bootstrap resampling method is used to simulate sampling distributions of the annual mean number of tropical cyclones for the above two batches individually. The statistical characteristics for the non–El Niño batch are very different from the El Niño batch.

A two-sample permutation procedure is then applied to conduct statistical tests. Results from the hypothesis testing indicate that the difference in the annual mean number of cyclones between El Niño and non–El Niño batches is statistically significant at the 5% level. Therefore, one may say with statistical confidence that the mean number of cyclones in the vicinity of Hawaii during an El Niño year is higher than that during a non–El Niño year. Likewise, the difference in variances between El Niño and non–El Niño batches is also significant. Cyclone tracks passing Hawaii during the El Niño batch appear to be different from those of the non–El Niño composite. A change in large-scale dynamic and thermodynamic environments is believed to be conducive to the increased cyclone incidence in the vicinity of Hawaii during an El Niño year.

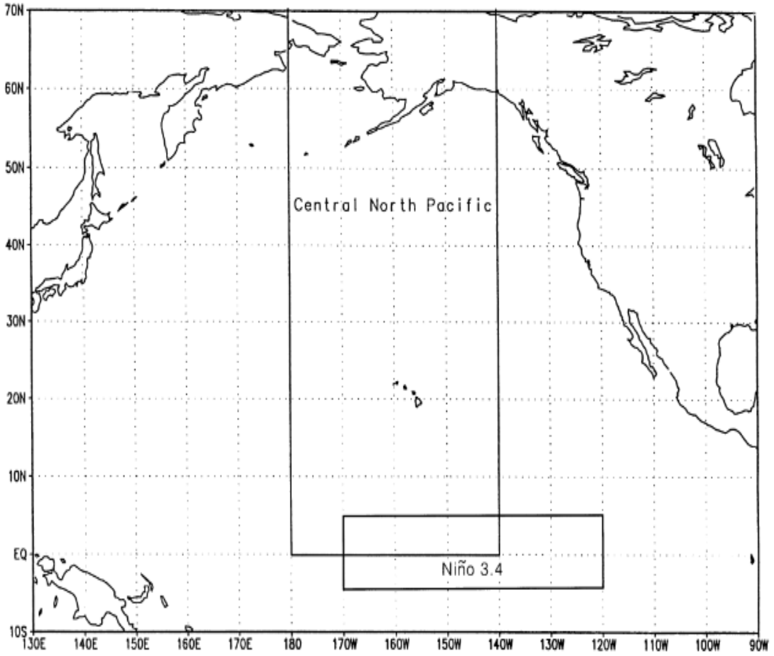

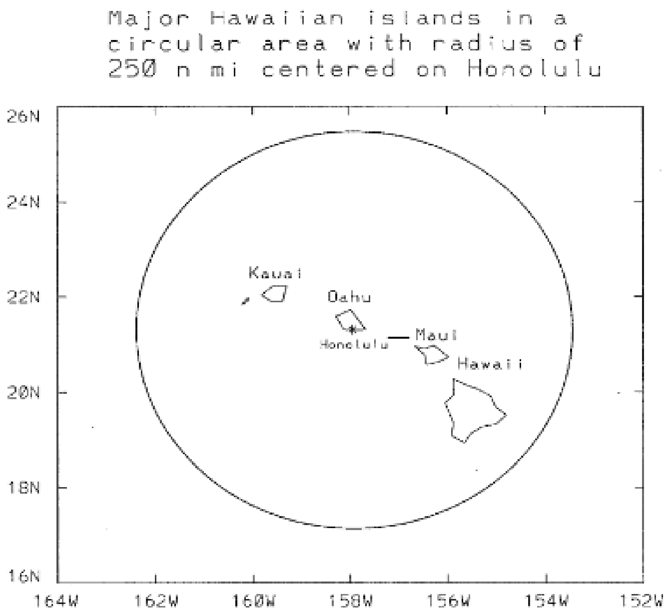

FIG. 1. Map of the major Hawaiian islands and the scan radius of 250 n mi from Honolulu.

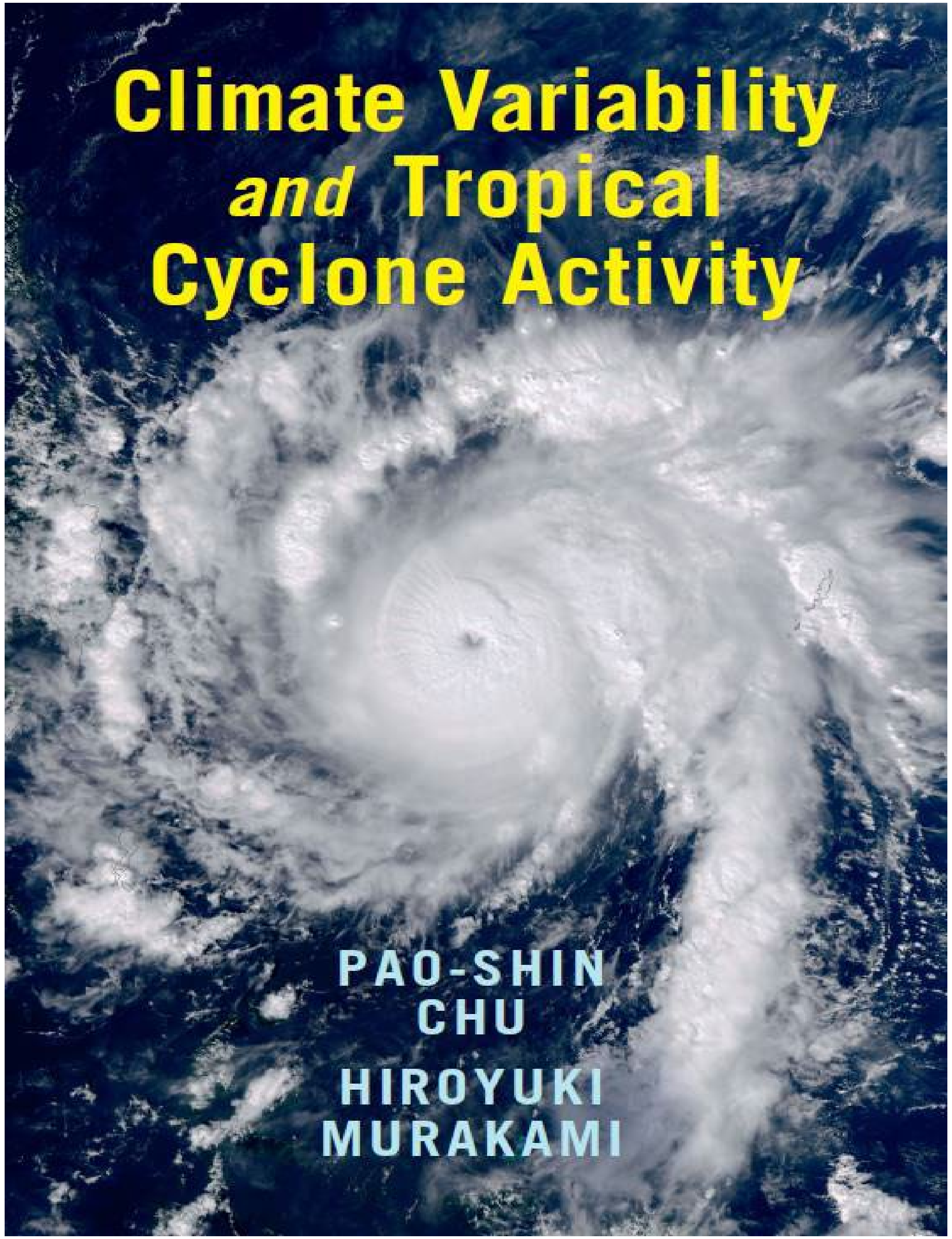

This book covers the fundamental theory, statistics, and numerical modeling techniques used when considering climate variability in relation to tropical cyclone activity such as shifting formation location, frequency of occurrence, storm tracks, landfall locations, intensity, and lifespan in the Pacific (western North Pacific, eastern North Pacific, central North Pacific, South Pacific) and Atlantic Oceans. Major climate modes that modulate tropical cyclone activity include El Niño and La Niña, Madden-Julian Oscillation, Pacific Meridional Mode, Pacific Decadal Oscillation, and others. There are 7 chapters. Particular attention is paid to projecting future tropical cyclone changes in response to increased concentrations of greenhouse gases.

Chu and Murakami, 2022, Cambridge University Press, 320 pp, available in Amazon.

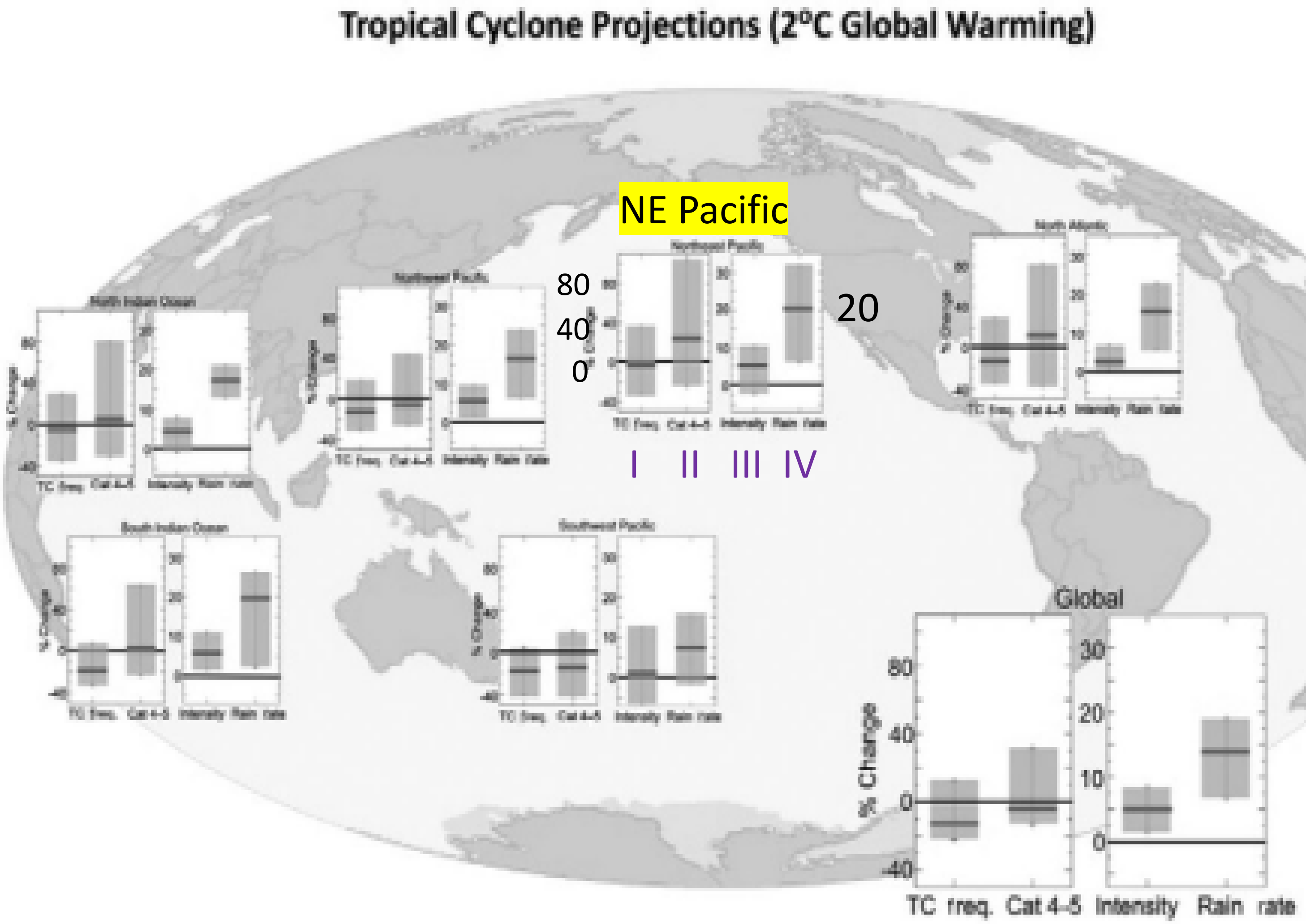

For Northeast Pacific, including Hawaii, there is essentially no change in annual storm number, but a higher frequency (30%) for category 4 and 5 hurricanes; hurricane will become more intense and a lot more hurricane rainfall (20% more) for a 2°C warming in the future.

Summary of tropical cyclone future projections for a 2°C global anthropogenic warming relative to 1986-2005 (Knutson et al., 2020). Four metrics were used: percentage change in (I) the total annual frequency of tropical storms; (II) annual frequency of category 4 and 5 storms; (III) mean Lifetime Maximum Intensity (LMI); and (IV) precipitation rate within 200 km of storm center at the time of LMI. The solid line in the box is the median of the expected percentage change, and the gray bar is the 90% (likely) confidence interval for storm frequency, and 80% interval for other three metrics. **Chu/Murakami, 2022**

Annual mean TC frequency

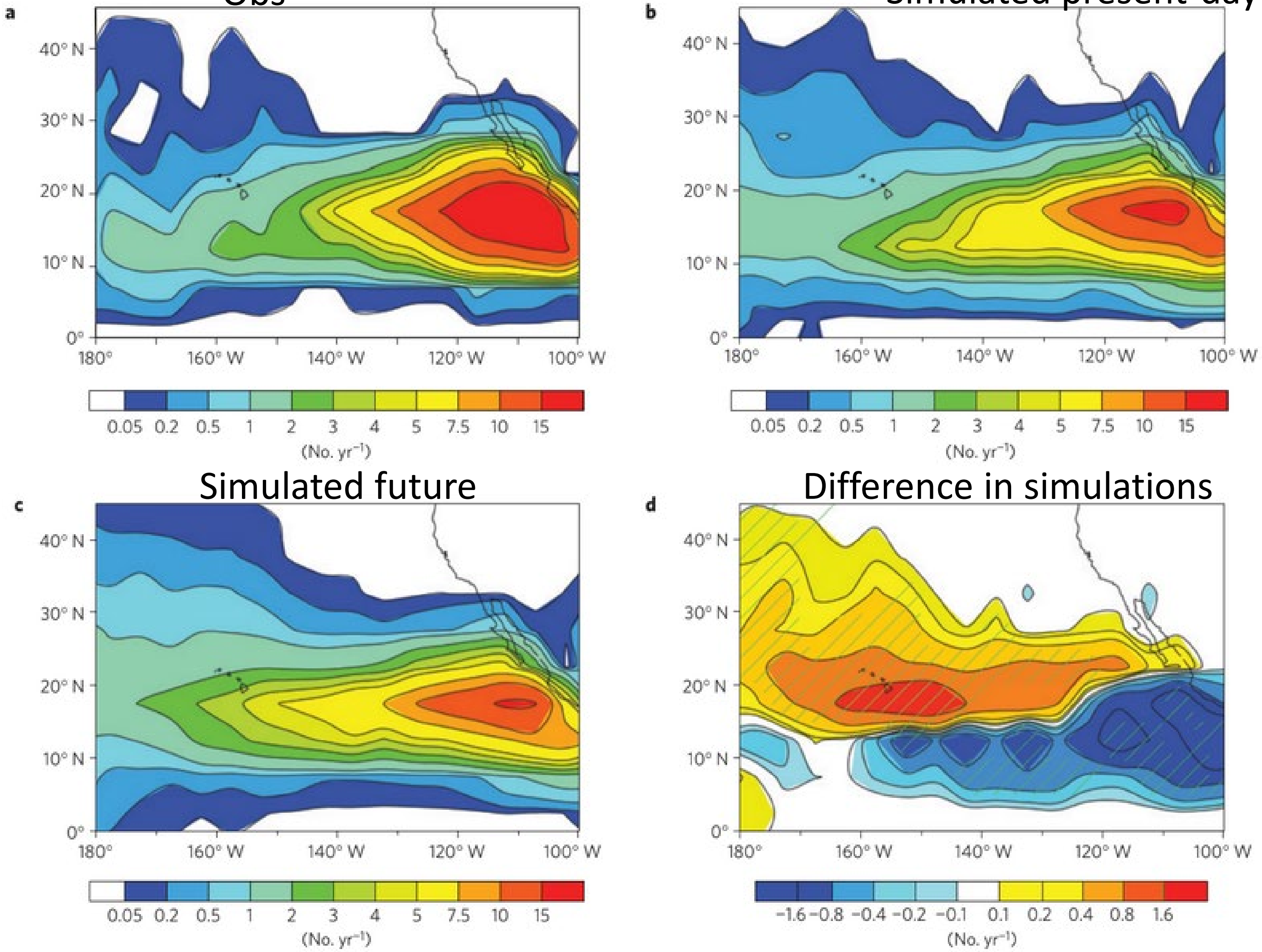

Figure 1 | Annual mean of TCF (number per year, colour scale) counted at every 5° x 5° grid cell. a, Observations (1979–2003). **b**, Ensemble mean of present-day experiments (1979–2003). **c**, Ensemble mean of future experiments (2075–2099). **d**, The projected future change. The green hatching indicate statistical significance at the 99% confidence level or above (by the bootstrap method) and give an indication of the robustness, with 8 of the 11 future experiments predicting mean changes of the same sign.

High-resolution atmospheric GCM

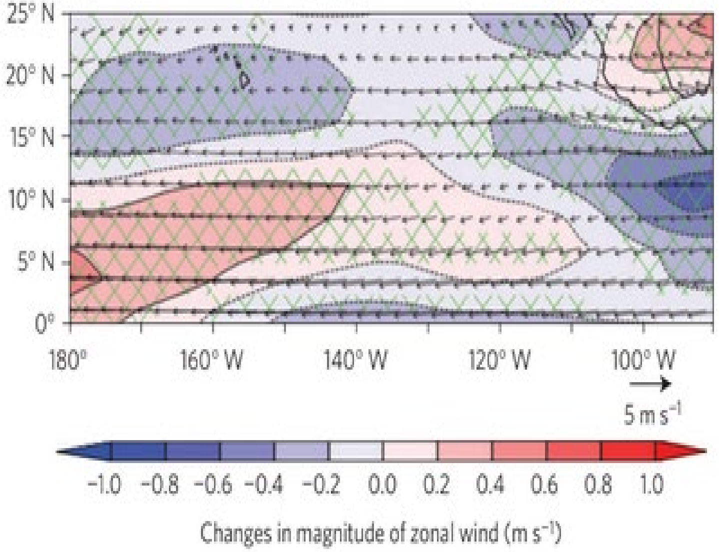

Figure 3 | Simulated mean steering flow during July–October. Superimposed are simulated mean steering flow for the 5 present-day experiments (vectors) and projected future changes in zonal component of steering flow for the 11 future experiments (colour shading; $m\,s^{-1}$). The green crossed lines indicate statistical significance and robustness as in Fig. 1.

A substantial increase in the likelihood of tropical cyclone frequency near Hawaii in the future (2075-2099) relative to the present-day climate (1979-2003).

Murakami et al., 2013

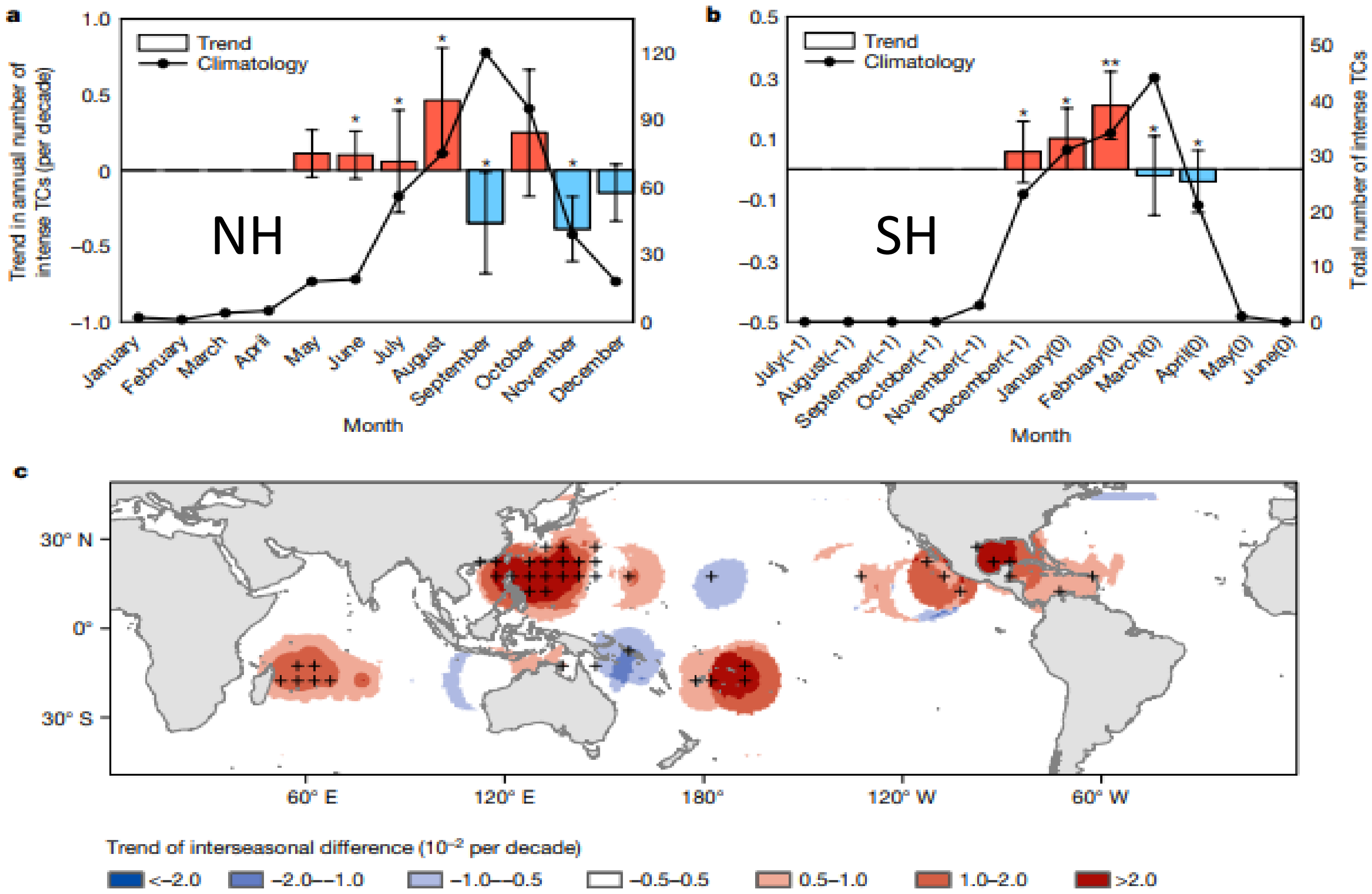

Linear trends of the interseasonal difference in intense TC numbers between the early and late seasons from ADT-HURSAT dataset. Black crosses denote significance. Positive (negative) trends in red (blue).

Shan, Lin, Chu, Yu, and Song, 2023, Nature, 623, 83-89.

Climatologically, intense TCs (cat 4-5) peak in autumn (September in NH and March in SH). The seasonal cycle of intense TCs lags behind that of other high-impact weather systems (e.g., summer monsoon rainfall), which often peak in summer (usually they are off by one season).

Increased (decreased) intense TC occurrence in the early (late) season.

Shifts toward earlier onset are evident in the WNP, ENP close to the Mexico coast, the Gulf of Mexico, the Caribbean Sea, southeast U.S. coast, South Indian Ocean and South Pacific near Fiji and Tonga. Shifts toward later onset (in blue) are observed over the central Pacific and near the Solomon Islands but they are not significant.

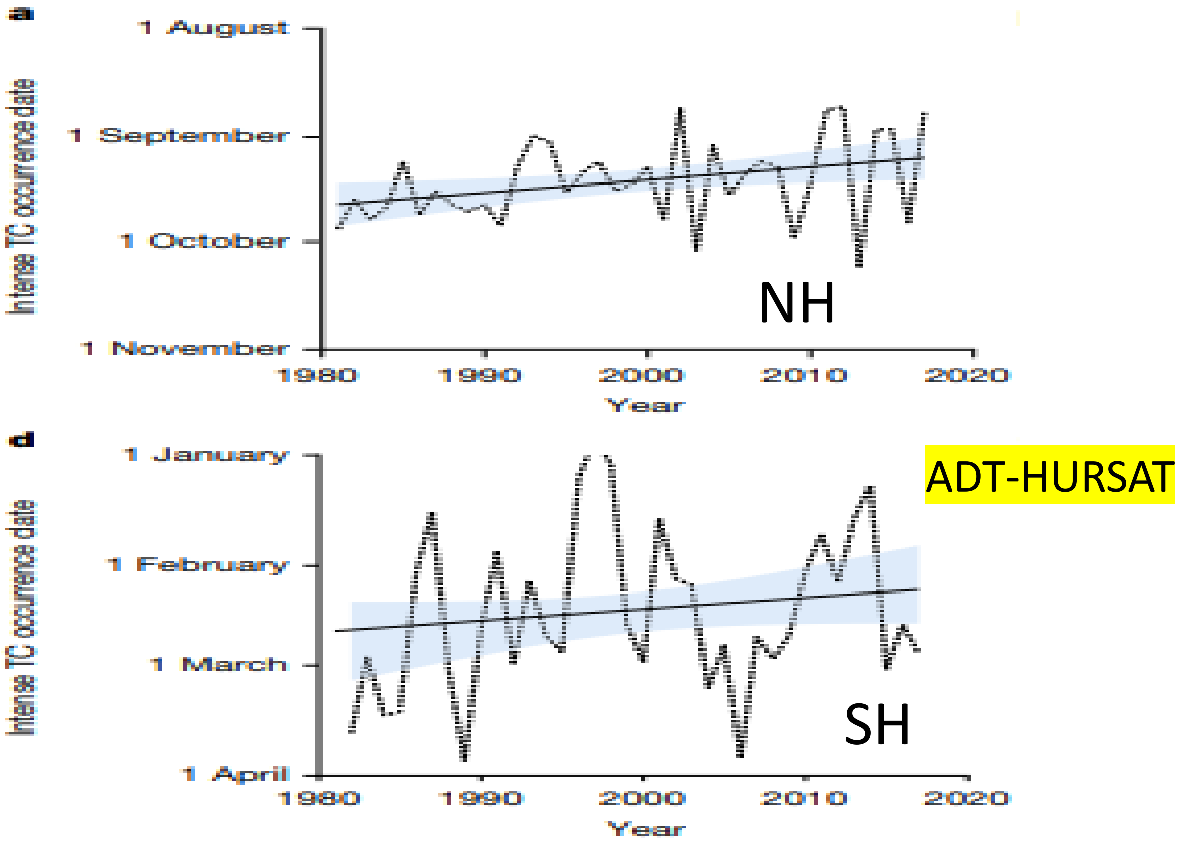

Time series of the yearly **median value of intense TC occurrence time** from 1981 to 2017 in the NH (a) and SH (d) from the ADT-HURSAT. Linear trends are significant at the 95% confidence level based on a nonparametric test. Shaded areas denote the 95% confidence intervals.

Intense TCs have been arriving three to four days earlier with each passing decade since 1981. This signal is also shown in the SH.

The overlap period in extreme rainfall from intense TCs and other weather systems is expected to be shortened.

This overlap could create devastating impacts of the compound hazards that are well beyond any one of these events individually. They can induce substantial inland rainfall, flooding, destructive wind, and fire associated with multiple weather systems, causing large-scale failures of power and transportation systems, straining emergency responses and depleting disaster preparation resources.

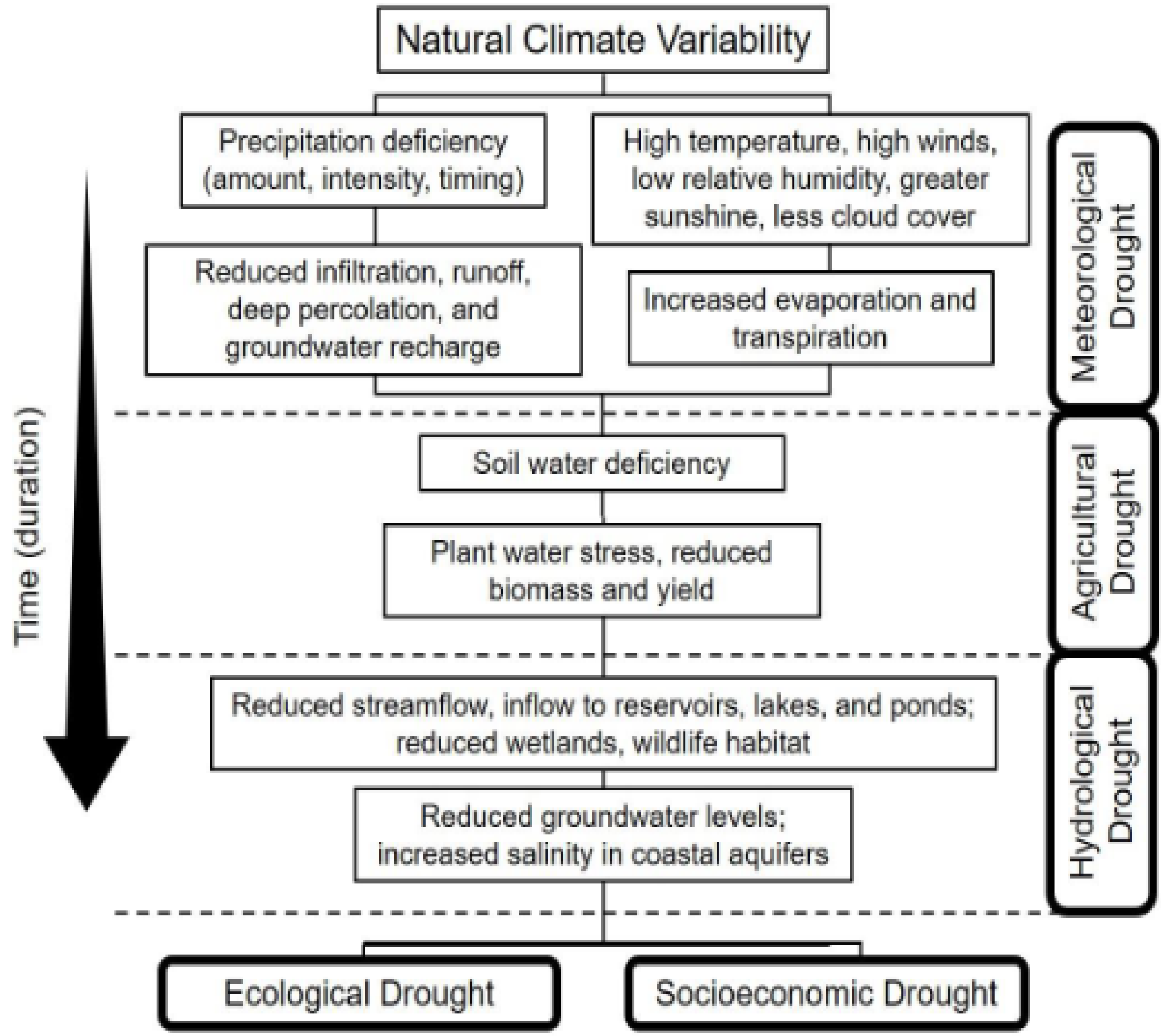

Figure 1. The general sequence for the occurrence and effects of different drought types (adapted from the National Drought Mitigation Center; https://drought.unl.edu/ (accessed on 7 August 2022)).

Hawaii Rainfall Index (HRI)

Chu and Chen, 2005

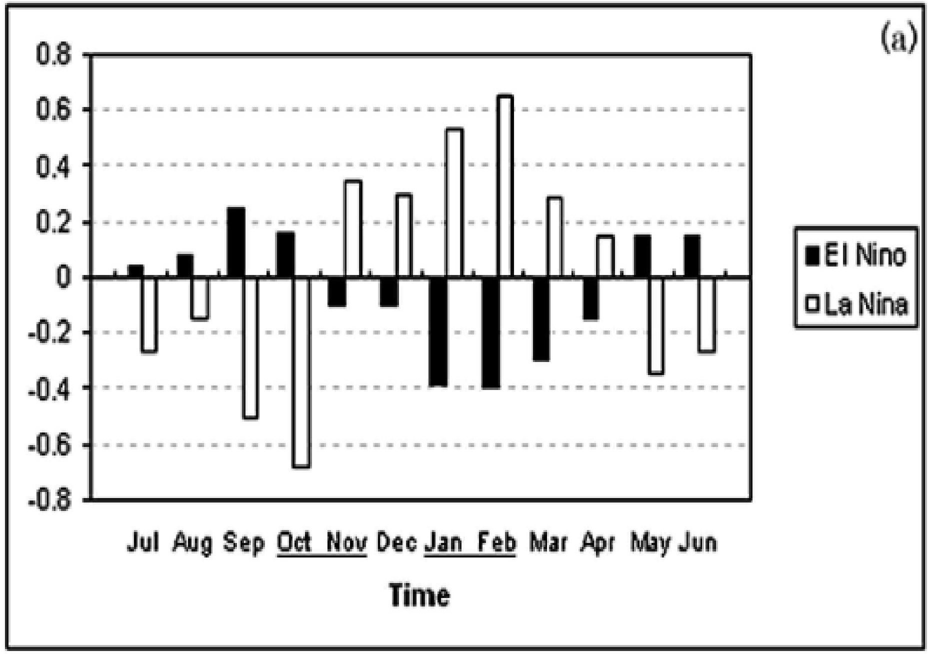

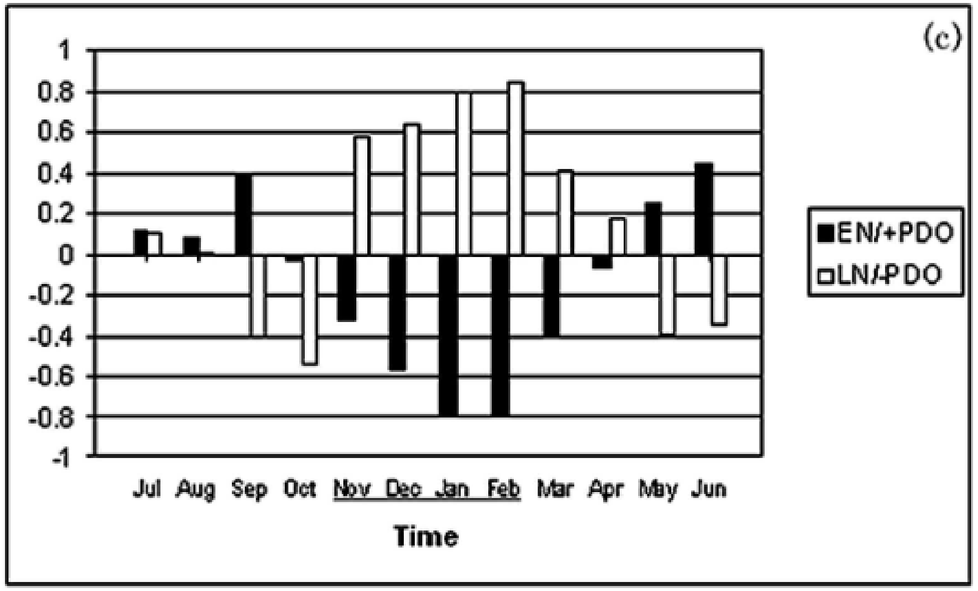

PDO: Pacific Decadal Oscillation

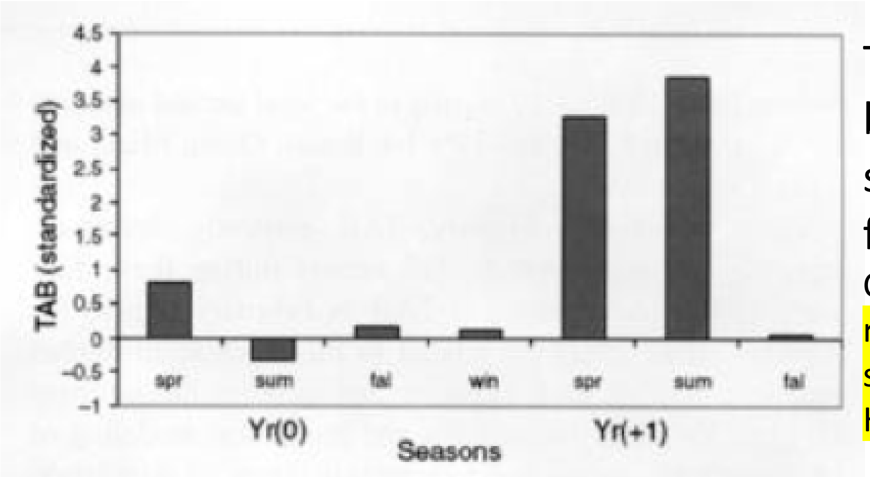

Fig. 4. Seasonal composite of Total Acres Burned (TAB) for Oahu during the four ENSO events (1976–1977, 1982-1983, 1986–1987 and 1991–1992.

Data from DLNR, Division of Forestry and Wildlife, 1976-1997.

Total acres burned (TAB) by wildfires for spring and summer are larger following an El Niño event.

Chu et al., Fire-climate relationships and long-lead seasonal wildfire prediction for Hawaii. Int. J. Wildland Fire.

Summer TAB prediction using the previous winter climate data and a nonlinear regression model for 4 islands.

Table 6. Logistic classification table for the summer TAB prediction for various islands in Hawaii with the 75th percentile (Q75) as the cut-off

The SOI of the preceding winter is the predictor variable

	Observed event	Correctly classified event	Observed non-event	Correctly classified non-event	Sensitivity (%)	Specificity (%)	Overall correctness (%)
Kauai	5	5	12	4	100	33.3	52.9
Oahu	6	5	16	14	83.3	87.5	86.4
Maui	6	3	16	5	50	31.3	35.4
Hawaii	6	3	16	7	50	43.8	45.4

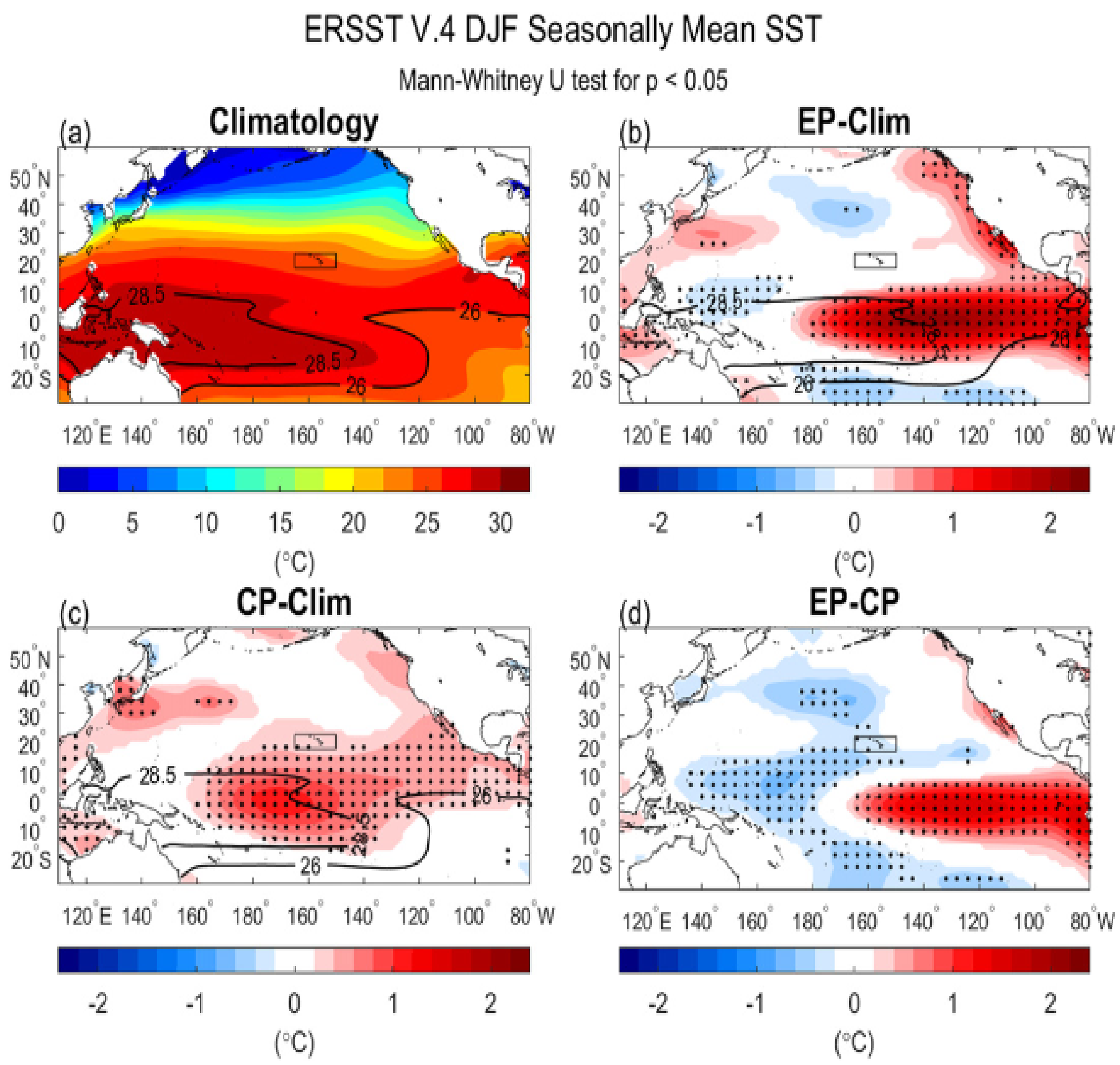

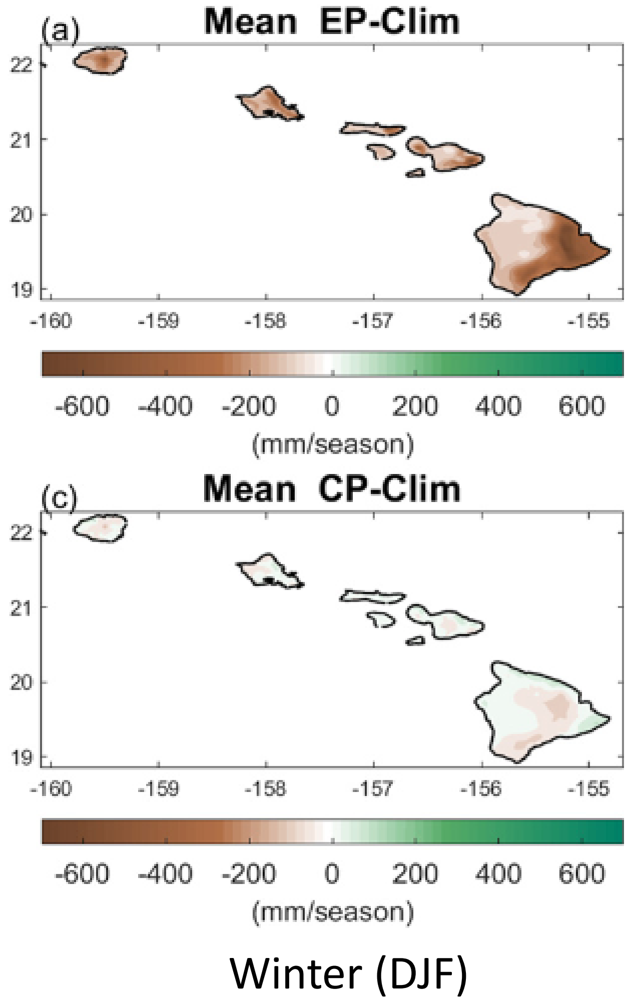

Lu, Chu, Kim, and Karamperidou, 2020, J. Climate.

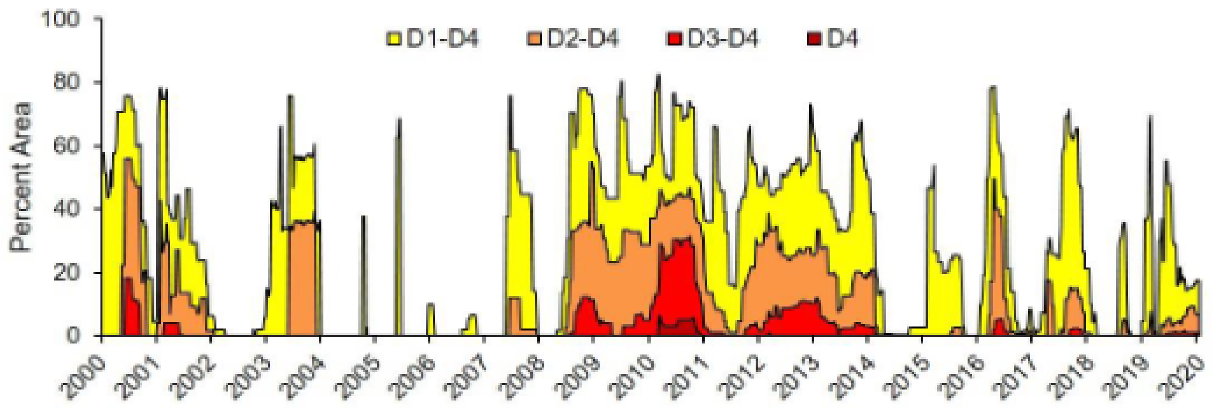

Figure 2. Hawai'i State Drought Monitor percent area time series, moderate drought (D1 category) or worse, from January 2000 through December 2019. D2 corresponds to severe drought; D3 to extreme drought; and D4 to exceptional drought. Data source: https://droughtmonitor.unl.edu/ (accessed on 30 August 2020).

D1: moderate drought (yellow)
D2: severe drought (orange)
D3: extreme drought (red)
D4: exceptional drought (dark red)

The percent area of drought is high from 2009 to 2014 (60-80%), and is pretty severe too. Hawaii State Drought Monitor.

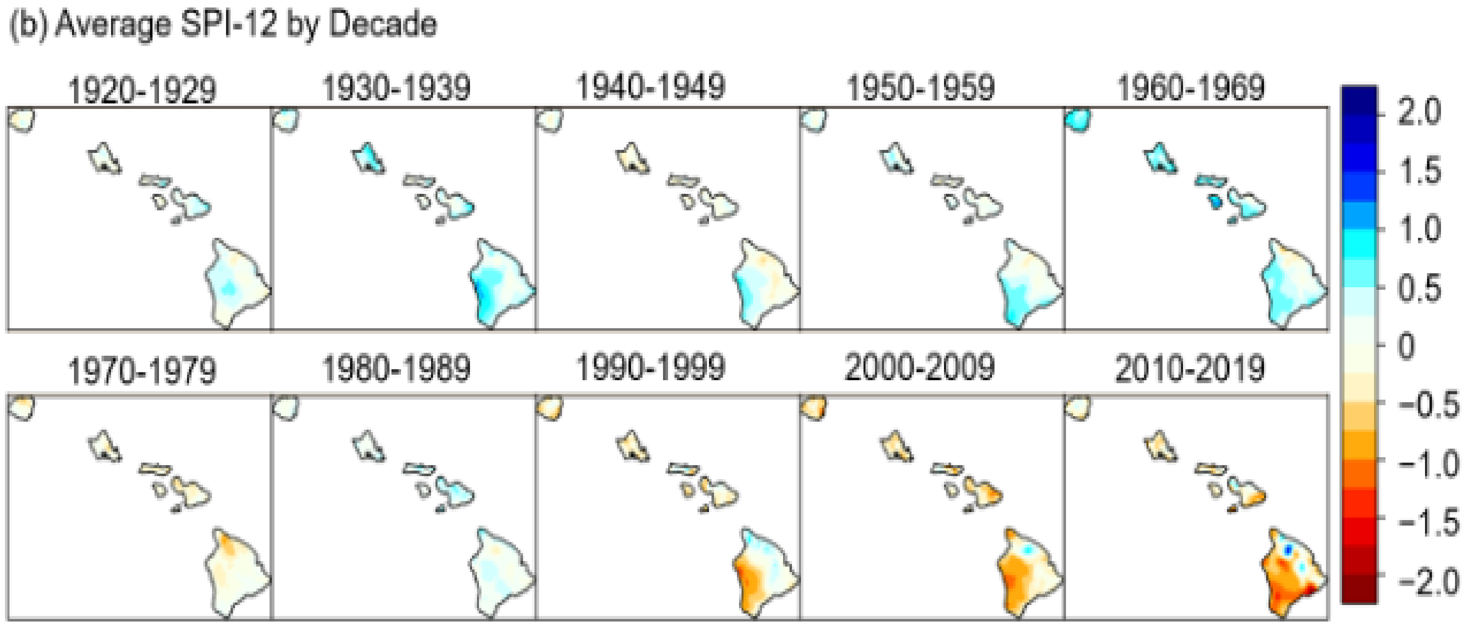

Average 12-mo Standardized Precipitation Index (SPI) by decade since 1920 (Frazier et al., 2022).

SPI <-1, moderate drought
SPI < -1.5, severe drought
SPI <-2.0 extreme drought

Future rainfall projection

- Statistical downscaling of rainfall changes in Hawaii based on 32 CMIP5 models for two scenarios (RCP4.5 and RCP 8.5) suggests that the wet regions on the windward slopes of the mountain regions are expected to be wetter in their seasonal mean precipitation amounts (2041-2071 relative to 1975-2005). For the dry leeward sides of Kauai, Oahu, Maui, and Hawaii, future precipitation exhibits the strongest drying trend (Timm et al., 2014).

- Dynamical downscaling (3-km resolution) based on 20 CMIP3 models reveals that wet windward sides will receive more rainfall, while the dry leeward sides will see less clouds and rainfall (2080-2099 relative to 1990-2009, Zhang et al., 2016).

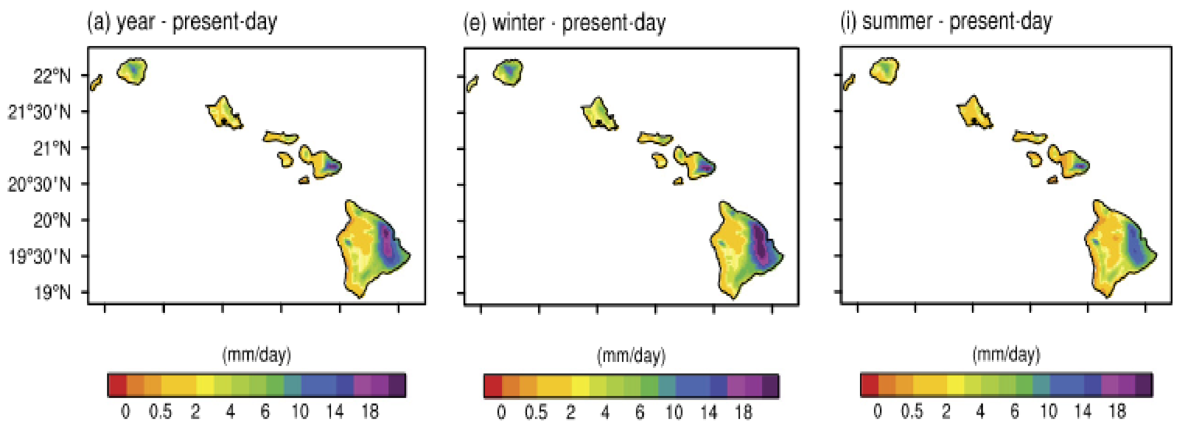

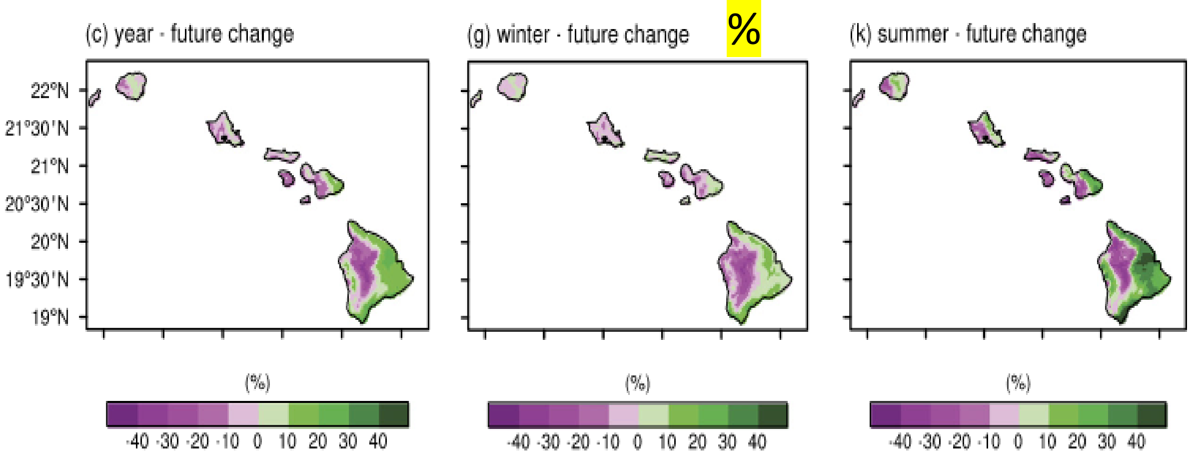

Summary

- Major climate modes modulates hurricane activity
- Generally, more hurricanes near Hawaii during El Niño years
- Higher number of intense hurricanes (cat 4/5) over the eastern/central North Pacific in the future for a 2°C warming; more hurricane rainfall in the future too
- Substantial increase in TC frequency near Hawaii in the future
- Intense TCs occurred earlier than before and may cause more compound hazards
- El Niño leads to dry winter and spring in Hawaii, which then causes more acres burned by wildfire in spring and summer; long-lead prediction of wildland fire is promising
- Drought became more widespread and intense in the most recent decades (2000-2009 and 2010-2019), particularly eastern Maui and the Island of Hawaii
- Projection of future rainfall using high-resolution CMIP6 models?